Econophysics: Agent-based modelling of Brownian motion and Kinetic theory of gases for markets and wealth distributions

2364784W

Abstract. Application of physics concepts and methods to economics has been fundamental to a number of its disciplines, with the recent popularisation of agent-based modelling techniques for studying economic systems. Stochastic physical systems such as Brownian motion, have been adapted to study economic applications, with Geometric Brownian motion serving as a foundation for modern stock price fluctuation models. A 2D kinetic theory of gases model was developed to understand the underlying mechanisms behind the random behaviour of gases and to support the development of a pseudo-2D equivalent for studying economic systems. Homogeneous and heterogeneous saving parameters were introduced to the model to study the impact of saving and unfair transactions on wealth distributions. Homogeneous saving parameters led to narrow Maxwell-Boltzmann-like wealth distributions with less inequality, whereas heterogeneous saving parameters made interactions more realistic; where individuals with higher saving parameters profiting off those with lower saving parameters, resembling businesses profiting off other businesses and individuals within society. Some of the resulting wealth distributions exhibited a "Pareto" power law relationship as is found in real societies throughout history. This highlights the importance of this work, developing an understanding of the relationship between money exchange and inequality within the modern world, with the potential to help guide future economic policy. Future research could explore this relationship further through real physical systems that exhibit power law relationships such as relativistic gases (i.e. cosmic ray spectrum), or driven systems studying a similar model but incorporating the constant production of money within economies and examining the impact of this on inequality.

1. Introduction

Money has played an integral role in the development of human society. It allows the indirect exchange of goods and services, enabling quicker and more flexible trading by acting as an intermediary and store of value. In the modern day, goods and services are traded between countries and on markets that are accessible to billions of actors (individuals and businesses) around the globe simultaneously through the internet, amounting to a multi-trillion-dollar worldwide economic system with innumerable intricacies and complex behaviour. The field of economics attempts to understand these behaviours for various purposes [1].

To understand these complex systems, economics has developed theories and sophisticated formulae to varying success. The lucrativeness and mystery surrounding this activity has attracted the interest of various physicists. Newton, Mandelbrot, and Gellman have famously had an impact on the field [2, 3, 4]. Whilst not originally termed econophysics until the mid-1990s, the process of applying concepts and methods used to study the physical world, to the complex structures seen in economic systems has been relevant throughout history and continues to find applications; evidenced by the recent PhysicsWorld front cover Figure 1. One might expect disparities between the idealised physics models of approximated, frictionless worlds, however, a more in-depth comparison between physics and economics reveals numerous analogies [5].

Some popular examples include that of Brownian motion, originally used to describe the random motion of physical particles in a fluid. This has contributed a fundamental part of stochastic finance, incorporated into several economic models to mimic the random variation of prices in markets; famously used to describe the underlying price of an asset in the Black-Scholes theory of option pricing, a widely used model for prediction of the price of an asset e.g. to price options contracts [6]. Other applications of physics to economics include: ideas of gravity being used to model international trade [6], chaos theory, quantum mechanics in quantum finance [7], and mechanics/kinetic models of trade [5].

Thanks to the rapid development of computational power and methodologies, computer modelling of complex systems has become a viable means for predicting and understanding their properties. This has particular benefit to economics, where many descriptions of systems are not analytically tractable and thus cannot produce numerical solutions.

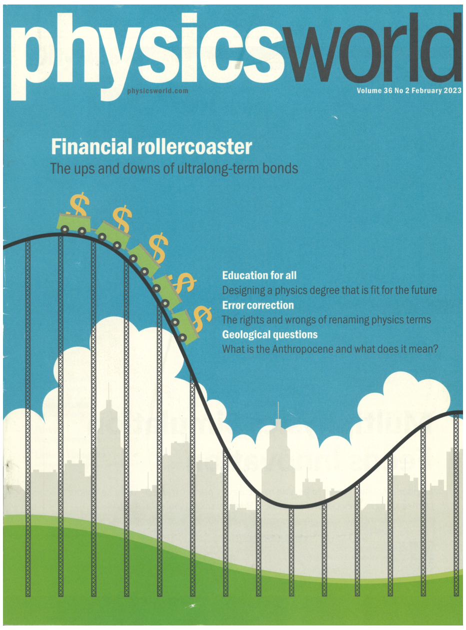

Figure 1: Recent front cover of Physics World magazine volume 26, No 2 February 2023 [8]

Agent-based modelling (ABM) is a modern computational method of modelling macroscopic systems from the interactions of its microscopic agents and has proven to be a powerful tool in contrast to the popular equation-heavy approach of economics. ABMs model large populations of interacting agents with simply defined behaviours, collectively producing complex emergent phenomena. These methods do not rely on the development of equations and can have vastly shorter computation times than the algorithms used to solve these equations [9]. The generalised process by which they function is illustrated in Figure 2. The behaviour of these agents refers to how they act and interact based on a number of factors that can include their environment, other agents, and their own attributes.

A popular physical application of agent-based modelling is the Ising model, a mathematical model describing the temperature dependence of ferromagnetic behaviour. The collective ferromagnetism is a result of the alignment of interacting magnetic dipoles within a lattice competing with the random reorientation of the dipoles due to thermal energy. This creates a non-trivial dynamic between this reorientation and the opposite ordering alignment of dipoles. The temperature at which the phase transition from order to disorder can be challenging to accurately predict, often depending on a number of system-specific parameters. Modelling this system using agent-based modelling is often a more accurate method of predicting this temperature, also allowing exploration of the effects of different parameter values [10]. Similarly, in economics, there are many theorems and corollaries that are not analytically tractable for which agent-based modelling provides an alternative to the common equation-heavy approach [5].

2. Brownian Motion

Brownian motion, named after the Scottish botanist Robert Brown who first noticed that small particles of pollen on the surface of water were in constant random motion. This stochastic behaviour has been observed and described for all size scales down to the atomic level. Mathematical formalisms of the concept of Brownian motion and "random walks" were developed by a number of scientists including Albert Einstein who explained the phenomena using statistical mechanics, attributing the motion to be a result of the collisions of particles within a fluid. His work provided a theoretical basis for the study of Brownian motion and acted as further evidence for the kinetic theory of heat and the second law of thermodynamics being statistical [11, 12].

Further applications of Brownian motion are extensive, particularly in economics owing to its random or stochastic behaviour, which can be seen in the pricing of assets in financial markets (e.g. stocks, bonds, and general items of value). The use of Brownian motion in these financial models, as in the famous Black-Scholes model, is based upon the presumption that the fluctuation of asset value is statistically random such that the random motion of particles can approximate microscopic changes in asset value. This presumption has subsequently been disproved, though it serves as a reasonable approximation under the efficient market hypothesis and is commonly used as a foundation for more complex financial models [14]. Stock markets mediate huge exchanges of assets, at profit and loss, between individuals vying to make more from their money. As such, methods to understand how stock prices are changing have been studied extensively for decades, with a range of techniques developed from mathematics, physics, and beyond. Brownian motion is one of the most popular examples of these techniques, to gain a better understanding of this, a Brownian motion model was developed.

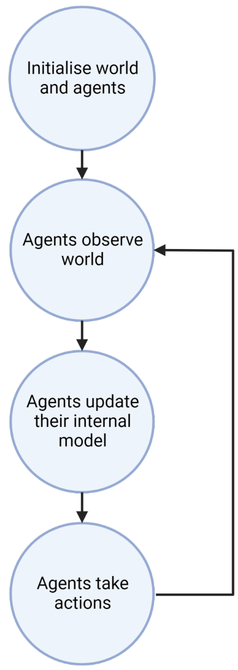

Figure 2: Diagram depicting the behaviour of agents in an agent-based model simulation [9, 13].

For general applications in financial modelling, it is common to use a simplified form of Brownian motion. This can be described by the fluctuation in position (or value an economic context), x, given by equation:

$$dx = \mu dt + \sigma r_n, \tag{1}$$

where dx is the change in position over a time step dt, μ the drift velocity, σ is the volatility of the system (related to the diffusion constant in physical Brownian motion), and r_n is a random number with mean $= 0$, and variance $= dt$. The growth of this model over time is simply μt and the variance of the growth $\sigma^2 t$.

Whilst simple Brownian motion captures the stochastic nature of stock price fluctuations, it lacks the overall trends of growth in economic markets. Geometric Brownian motion (GBM) is a prominent form utilised in financial modelling due to the scaling of its fluctuations and drift velocity exponentially with time. It takes the formula:

$$dx = x(\mu dt + \sigma r_n), \tag{2}$$

where the additional factor of the stock value scales both the drift velocity and volatility with the stock value. GBM also ensures positive values given a positive starting position, positive drift, and sufficient time which is a trivial restriction on stock prices. The growth of this model follows the relationship $x_0 e^{\mu t}\sqrt{e^{\sigma^2 t-1}}$ with its variance growing as $S_0^2 e^{2\mu t}\left(e^{\sigma^2 t}-1\right)$ [15].

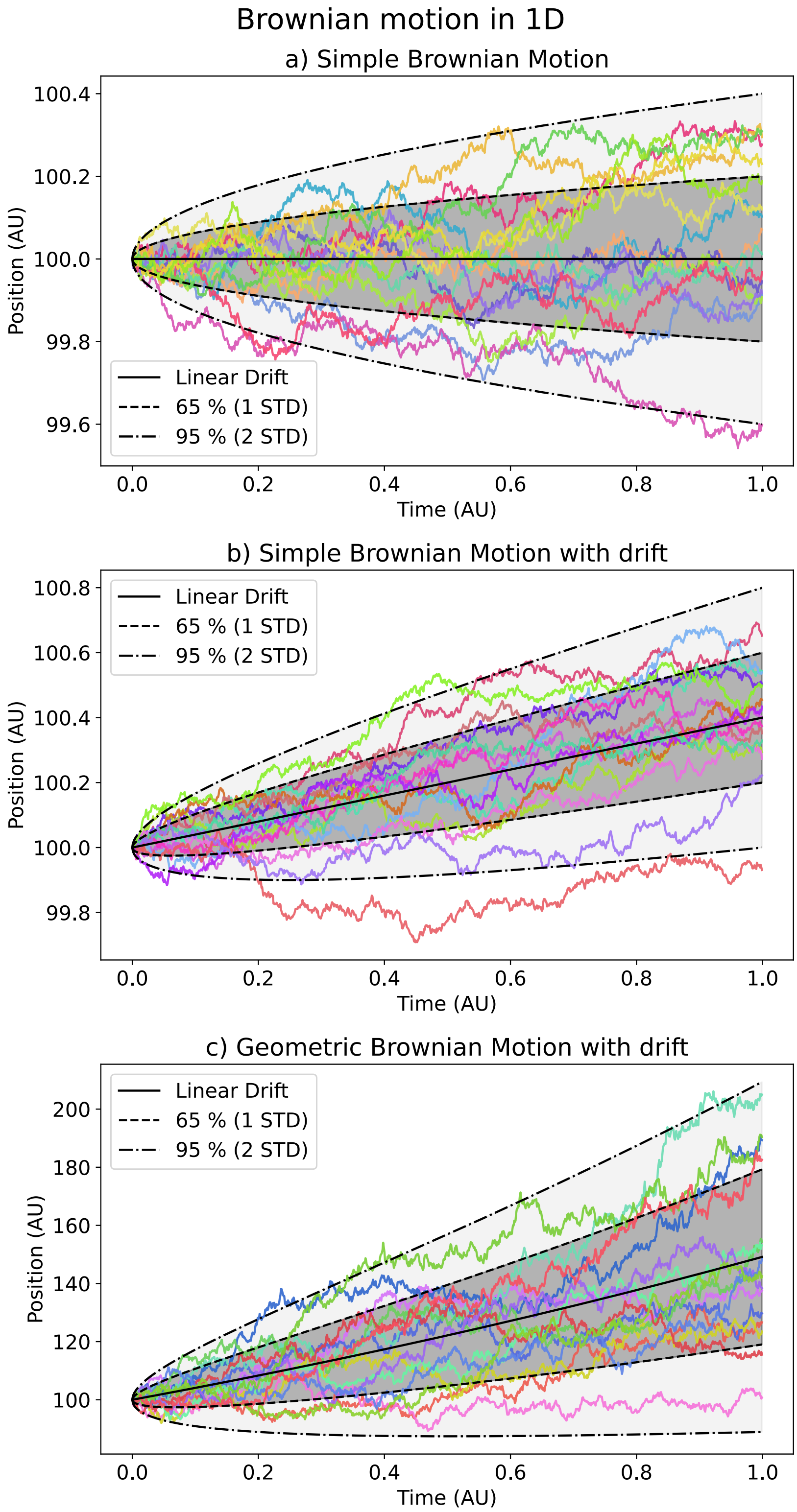

Figure 3: Depiction of various forms of Brownian motion in 1D. a) Simple Brownian motion with no drift. b) Simple Brownian motion with drift. c) Geometric Brownian motion with drift.

2.1. Method

The aforementioned mathematical descriptions were implemented into the behaviour of 20 agents, with arbitrarily chosen starting parameters. For reference these were: volatility (σ) = 0.2, drift velocity (μ) = 0.4, time step = 0.001, total simulation time = 1, starting position = 100. The positions of these agents were depicted with their expected growth and standard deviations to depict the spread of values. Source code is available with instructions in Appendix 8.9.

2.2. Results & Discussion

A set of simple Brownian random walks, without and with drift respectively, can be seen in Figure 3 a) and b). These illustrate the stochastic nature of Brownian motion and their resemblance to stock price fluctuations. Whilst the model with drift shows some growth, the trend is clearly stiffer than that of Geometric Brownian motion in Figure 3 c) which is growing exponentially more comparable to economic growth. Despite its similarities in shape to stock market fluctuations, GBM is a simplistic model with constant market parameters like drift velocity and volatility, conflicting with empirical evidence showing that volatility fluctuates and clusters [16], with overall market movements affecting the growth of the stocks themselves. More complex parameterised models are often built upon GBM to account for these effects, though this only detracts from the analytically tractable, purely stochastic nature of GBM.

In conclusion, Brownian motion is a fundamentally stochastic physical process occurring as a result of the random collisions of particles within a fluid. Understanding this behaviour mathematically, through studying the physical systems that exhibit it, has provided an invaluable tool for stochastic economics. For example, the study of stock price fluctuations, for which specific variations of Brownian motion are particularly common (i.e. Geometric Brownian Motion). Despite this, the advantages of Brownian motion as an analytically tractable, physically random process are insufficient for many economic systems due to their further complexity. As such, these models serve as components of more sophisticated economic models, such as the Black-Scholes model for option pricing. This highlights the relevance of random physical processes for economics, in particular those produced by microscopic kinetic interactions. The next chapter in this report will discuss the development of a kinetic theory of gases model with the intention of using them to study economic systems.

3. 2D Kinetic Theory of Gases

Whilst Brownian motion provides a means of predicting the random motion of particles, it merely encodes this through a random number with a defined variance. The physical process that encodes this property of Brownian motion is the random collisions of particles within that medium; driven by the inherent thermal energy contained within the system. This process was famously described by the kinetic theory of gases model which was formalised by Maxwell and Boltzmann forming one of the foundational concepts of thermodynamics [17]. To explore this stochastic physical system for understanding phenomena in economics, it was relevant to first develop the physical model, and then assess its relevance to economic systems.

The kinetic theory of gases is a bottom-up approach to understanding the macroscopic behaviour of gases and their thermodynamic properties by modelling the microscopic behaviour of individual gas particles at the molecular level. Through modelling the classical interactions between these particles, undergoing elastic collisions with one another, the kinetic theory of gases provides a theoretical framework for understanding the macroscopic properties of a gas, such as pressure, temperature, and volume. This theory has been fundamental in the fields of statistical mechanics and thermodynamics producing universal laws such as the ideal gas law, which relates the aforementioned macroscopic properties of a gas (PV = nRT), the concept of specific heat capacity, and also producing the Maxwell-Boltzmann distribution; which can

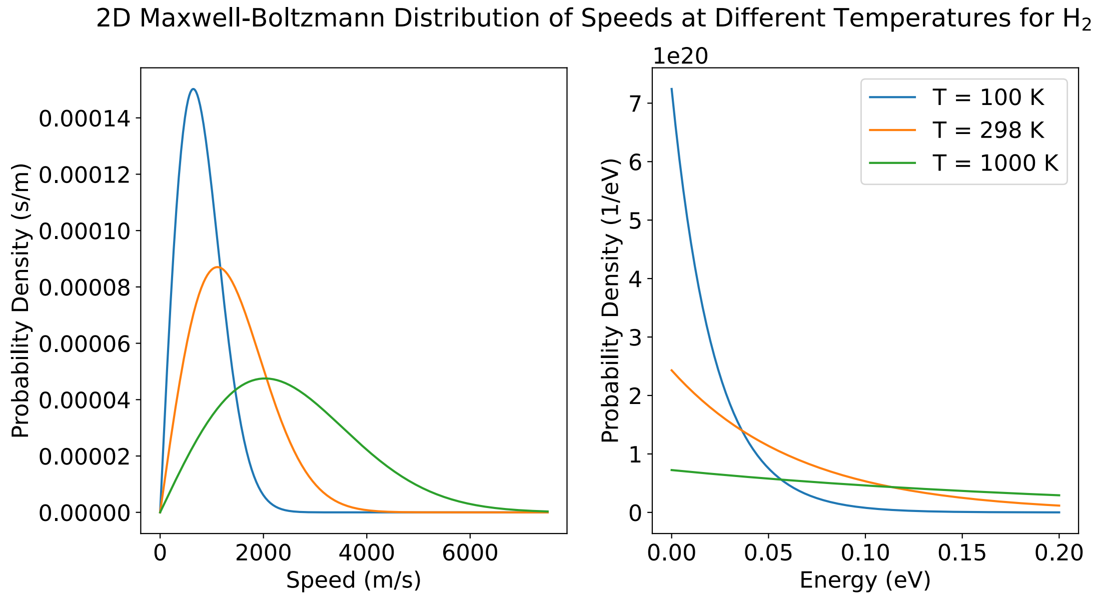

Figure 4: Two diagrams depicting the 2D Maxwell-Boltzmann a) speed and b) energy distributions at different temperatures for H_2.

describe the distribution of energy within an ideal gas and other thermodynamic systems.

The Maxwell-Boltzmann distribution is used to describe the distribution of energy within an ideal gas at thermal equilibrium and has shape depicted in Figure 4. However, the distribution can be used to describe other thermodynamic systems containing large numbers of randomly interacting particles so long as the required assumptions are met, with looser application in the field of economics [18]. An understanding of the distribution can be provided from its derivation. This begins through the application of the Boltzmann factor which defines the ratio of probabilities of two states based upon their energy and the temperature of the system:

$$f(E) = exp\left(-\frac{E}{k_b T}\right), \tag{3}$$

where E is the energy of the state, k_b is the Boltzmann constant, and T is the temperature of the system in Kelvin. The Boltzmann factor can be converted into a probability distribution, more specifically the Maxwell-Boltzmann distribution through normalisation:

$$P(E) = \frac{exp\left(-\frac{E}{k_b T}\right)}{Z}, \tag{4}$$

where Z is a normalisation factor given by the partition function which sums the Boltzmann factor for all possible states like so:

$$Z = \int_0^\infty exp\left(-\frac{E}{k_b T}\right) dE. \tag{5}$$

Combining these gives a final Maxwell-Boltzmann energy distribution of:

$$P(E) = \frac{exp\left(-\frac{E}{k_b T}\right)}{\int_0^\infty exp\left(-\frac{E}{k_b T}\right) dE} = 2\sqrt{\frac{E}{\pi}}\left(\frac{1}{k_b T}\right)^{\frac{3}{2}} exp\left(-\frac{E}{k_b T}\right) \tag{6}$$

The equivalent Maxwell-Boltzmann speed distribution can be further derived by defining particle energy as kinetic energy $\frac{1}{2}mv^2$, using the magnitude of the velocity vector adapted to 3 Dimensions $v = \sqrt{v_x^2 + v_y^2 + v_z^2}$. Including normalisation constants gives a final speed distribution:

$$P(v) = \left(\frac{2}{\pi}\right)^{\frac{1}{2}} \left(\frac{m}{k_b T}\right)^{\frac{3}{2}} v^2 exp\left(-\frac{mv^2}{2k_b T}\right), \tag{7}$$

where h is Planck's constant, and m is the mass of the particle. Finding the average of this distribution provides another key result, with an average velocity of $\frac{3}{2}k_b T$ demonstrating the equipartition theorem which states that, for every degree of freedom of the gas particles, the particle contributes an average energy of $\frac{1}{2}k_b T$ to the total energy of the gas [19]. Note that the speed and energy distribution must be adjusted for 2-Dimensions for the subsequent models, utilising $v = \sqrt{v_x^2 + v_y^2}$ with the speed distribution taking the new form:

$$P(v) = \left(\frac{m}{\pi k_b T}\right) v exp\left(-\frac{mv^2}{2k_b T}\right). \tag{8}$$

Subsequently, the 2D Maxwell-Boltzmann energy distribution can be derived from this, detailed in Appendix 8.1, giving:

$$P(E) = \frac{1}{k_b T} exp\left(-\frac{E}{k_b T}\right). \tag{9}$$

Foundational to the kinetic theory of gases model is the elastic collision. At its core, an elastic collision involves the exchange of momentum and energy between two interacting particles according to the universal conservation laws:

$$m_1 u_1 + m_2 u_2 = m_1 v_1 + m_2 v_2, \tag{10}$$

for momentum, and

$$m_1 u_1^2 + m_2 u_2^2 = m_1 v_1^2 + m_2 v_2^2, \tag{11}$$

for energy, where u_i are initial velocities and v_i are final velocities, and m_i are masses of the particles. The models employed in this thesis assume identical particles, thus identical mass. Consequently, in a 1D collision, the momenta and energies of the particles are completely exchanged (i.e. $u_1 = v_2, u_2 = v_1$). Expanding to further dimensions, one must consider the relative positions of the particles at the point of contact. By separating the particle velocities into components parallel and perpendicular to the collision vector (vector between the centres of the particles), a 2D or 3D collision is reverted to a 1D collision involving the parallel components, with perpendicular components unaffected. In practice, the method utilises a rotation of the frame of references to isolate the parallel velocity components for calculation of collision dynamics as illustrated for 2-Dimensions in Figure 5.

This highlights the simplicity of the function of elastic collisions as energy transfer mechanisms, where the exchange of momentum is entirely dependent on the collision vector with respect to the motion of the individual particles. This will be relevant for later models explored in this project.

3.1. Model & Method

A 2D kinetic theory of gases model was constructed using Python, and the Mesa agent-based modelling framework, along with scientific libraries such as numpy, scipy, matplotlib, seaborn, pandas, and ipywidgets for graphical user interfaces. The model was initialised with n non-overlapping spherical agents of radius r each with initial kinetic energy E, and uniformly randomised initial direction of velocity, all placed with a 2D NxN square of toroidal geometry. The model is progressed through time using discrete time increments, during which each agent followed the logic illustrated in Figure 6. First, the agent is moved forwards according to its velocity v, and time step dt. If the agent is moved past the edge of the toroidal square, it is mapped around the other side of the square. The agent then detects for collisions with a nearby

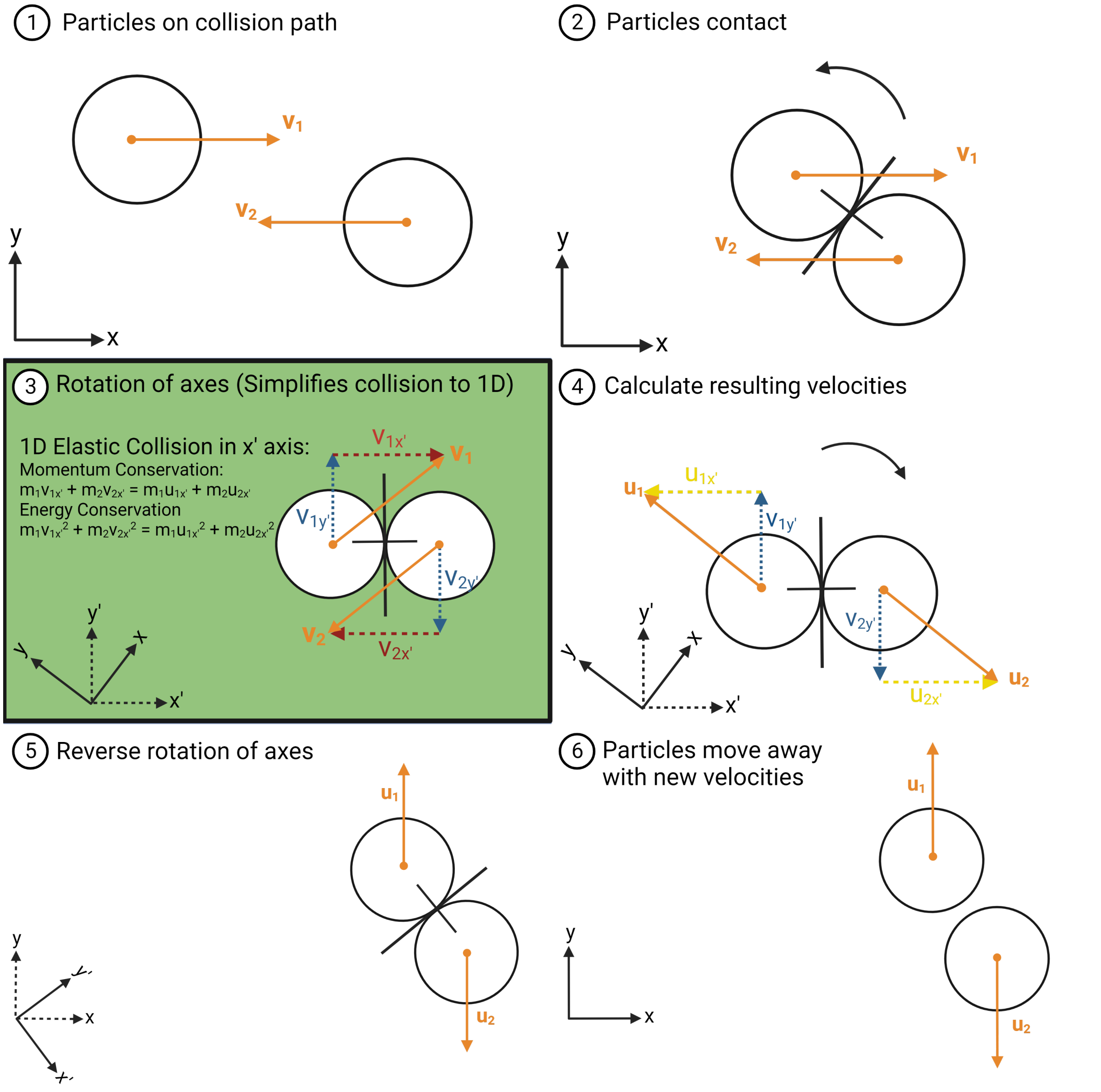

Figure 5: Diagram showing stepwise explanation of a 2D elastic collision of 2 identical spheres [13].

subset of agents. If a collision is detected, the elastic collision dynamics of that collision are calculated, then the agent is repositioned based on a corrected collision path. This process is completed for each agent in the population. After each time step, the simulation data including agent positions and velocities are collected for each agent for later visualisation and data analysis. A full simulation is run for a number of time steps.

The 2D gas model was visualised through a 2D positional plot of particles as spheres of colour corresponding to their speed. Speed distributions of the particles are plotted, using histograms or kernel density estimation (KDE), then fitted with a Maxwell-Boltzmann distribution. Speed distributions were chosen as they more clearly depict differences in shape than energy distribution. To identify the relaxation of the distribution into a steady state, the relative entropy statistical distance metric was used, explained in Appendix 8.5. The relative entropy was taken between a rolling averaged distribution over a 10-step window and an averaged distribution of the final 100 - 1000 steps. Due to space limitations, the results and implications of the relaxation are discussed in Appendix 8.2.

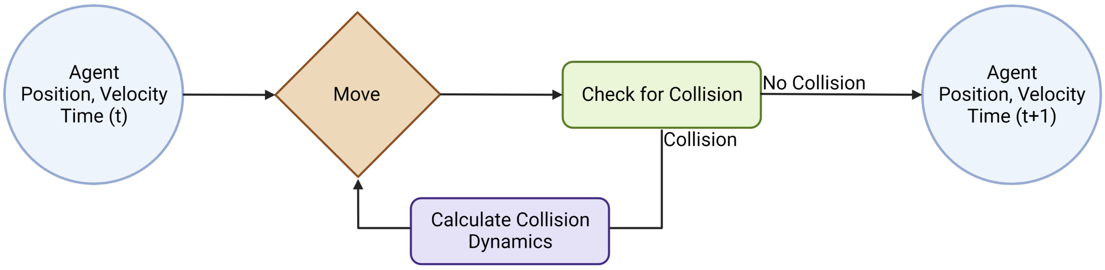

Figure 6: Flowchart diagram depicting the logic undergone by an activated agent in the 2D Kinetic theory of gases model [13].

Validation of the model was completed through various tests. Collision dynamics were tested first using pairs of agents, scanning through sets of collision angles, starting positions, and velocities. These models were scaled up in numbers of agents until the function of the model was decided to be satisfactory. The presented results use the model parameters unless otherwise stated: 1000 steps, 200 agents, 10 starting energy, a side length of 100, and a particle radius of 2. Source code is available with instructions in Appendix 8.9.

3.2. Results & Discussion

An example simulation was run, and its results are illustrated in Figure 7. The figure depicts initially uniform speed distribution between the particles, evidenced by the narrow spike in probability distributions in steps 1 a) and 10 b), and the generally unchanged colours and thus speeds of the particles in the positional plots. Subsequently, the uniform distributions relax into the steady-state Maxwell-Boltzmann 2D speed distribution depicted in step 1000 c) and reaffirmed by the diffuse spread of colours within the positional plot. The positional plots also depict the path of a particle throughout the simulation, showing a resemblance to a Brownian random walk in 2D. An animation of a comparable simulation is also available at url:2364784w.github.io. A separate, longer 5000-step simulation was run and fitted with a Maxwell-Boltzmann speed distribution to further demonstrate validity, and is available in Appendix 8.4.

The produced model has exhibited the expected phenomena of the kinetic theory of gases verified by fitting of characteristic Maxwell-Boltzmann distribution. More generally, the results revealed the nature of the random kinetic processes behind ideal gas systems; illustrating that despite the inherent stochastic behaviour of individuals within a kinetic theory model, emergent, collective phenomena are produced.

Despite this success, some flaws were identified during the development of the model. Explicit predicting of collisions was not incorporated into this model due to the computational cost of predicting collisions for large numbers of agents. Instead, the model detects collisions after the movement of particles, calculating collision dynamics upon detection of the collision. This workaround is functional on the basis that the ratio of velocity to time step is sufficiently small such that all collisions are detected and with approximately the correct geometry. This allowed a vastly reduced computation time which was desirable for this application. Further reasoning for this can be found in Appendix 8.3. Animated visualisations of this model are available at url:2364784w.github.io, acting as further evidence of accurate collision dynamics.

For the application of this 2D kinetic theory of gases to economic systems, one must consider the following limitations inherent to this model. One of the primary limitations is its dependence on geometry, where the interactions of particles depend on their path and immediate

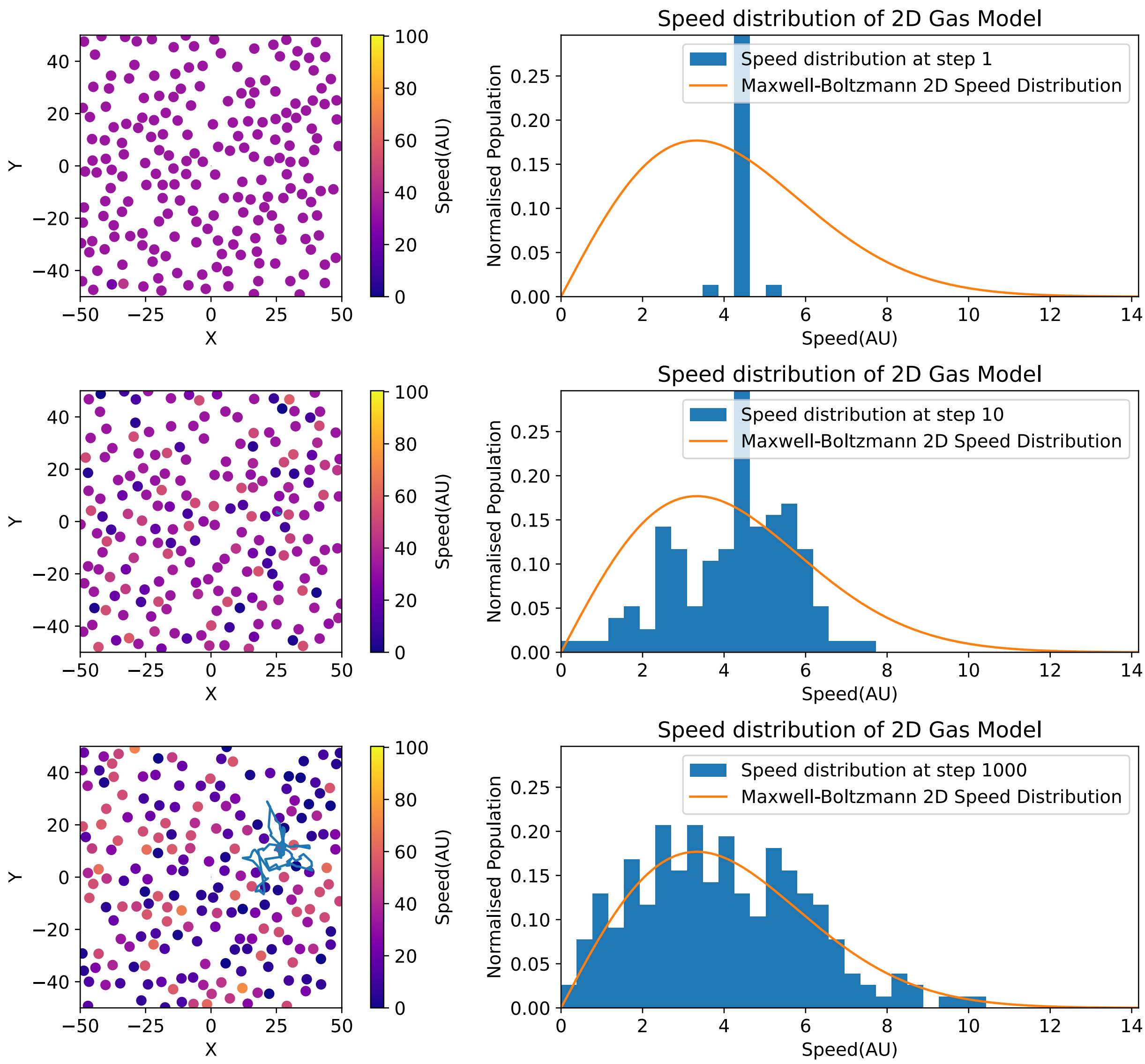

Figure 7: 3 rows of graphs depicting the 2D gas model positional plots and speed distributions at varying points in time: a) beginning (step 1), b) middle (step 10), and c) end (step 100) of the simulation. In the positional plots (LHS), particles are coloured based on their speed. A blue line depicts the random path of a single particle. In the probability distributions in speed (RHS), a histogram of the final step distribution is drawn, with a Maxwell-Boltzmann speed distribution fitted to a 100-step averaged final distribution. The speed distribution was clipped in a) and b), as full visualisation detracts from the redistribution of speed/energy.

surroundings. Whilst the model has inherent randomisation of interaction partners between local individuals, it limits the potential collision partners to a physical region based on the particle's velocity and the number density of the particles in the defined space. In many modern economic systems, interactions between agents can occur across vast distances instantaneously, thus the kinetic theory model in this form would not be suitable for these systems due to this geometric dependence.

Moreover, the prediction and calculation of collision dynamics can be computationally expensive when scaled up to large numbers of agents over large numbers of steps. This would limit the model to a relatively small number of individuals compared to real economic systems. Additionally, as mentioned previously, the collision detection methods assume a small ratio of velocity to time step. Scaled-up models with a larger number of agents have a greater probabil-

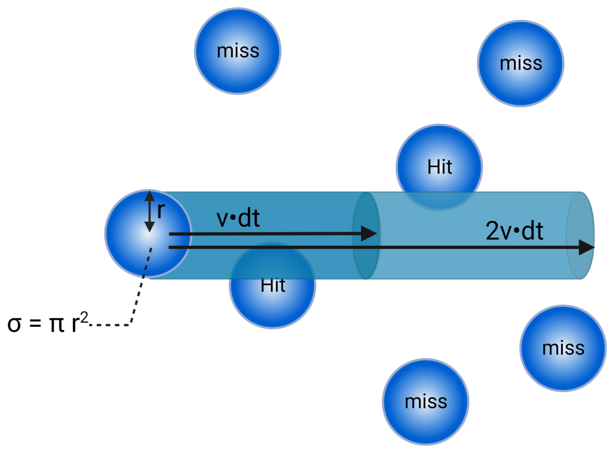

Figure 8: Diagram of depicting interaction volume of a spherical particle with velocity, v, radius, r, over time step, dt [13].

ity of agents taking up higher energies and velocities, thus the assumption to maintain realistic collision dynamics may not hold.

More generally, the 2D gas model presented in this thesis exhibits limited flexibility in adjusting interaction mechanism, restricting it to collision-like interactions to prevent unrealistic positioning of particles. While the geometric dependence of the model is not desirable for economic adaptation, it encodes two features that were predicted to be essential to the redistribution of energy in the kinetic theory model. Energy transfer through randomised collision geometry and inherent control over the number of collisions a particle undergoes depending on its velocity, shape, and size, referred to as collision frequency. Subsequently a pseudo-2D model was developed, designed to incorporate the two key parameters for energy redistribution, whilst extracting geometric dependence.

4. Pseudo-2D kinetic theory of gases model

Whilst a 2D kinetic theory model provides a true to reality physical description of the interactions of gas particles, the model is limited in its adaptability for use in study of economic systems. Most notably, it exhibits a geometric or spatial dependence that selects for local collision partners contrasting many modern economic systems in which near-instant transactions can occur irrespective of location. It also encodes a relationship between velocity and collision frequency, and randomises collision geometry thus energy transfer through 2D elastic collisions. To address these issues whilst retaining other characteristic properties, a pseudo-2D kinetic theory of gases model was developed.

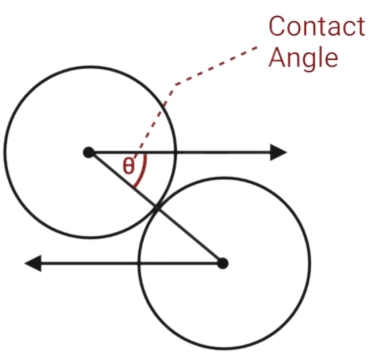

Figure 9: Diagram depicting contact angle in a 2D collision [13].

The concept of random selection of agents (e.g. selection of collision partners, or order of activation) is a critical aspect of agent-based modelling (ABM) as it helps to ensure that the model accurately reflects the underlying complexity of the system being modelled. In the pseudo-2D model, local geometric collision partner selection is substituted for random selection from the total population of agents.

The collision frequency (f) is a measure of the number of collisions that a particle undergoes per unit time. It depends on a number of properties including the number density of a system, its relative velocity, and its collision cross-section. These properties were intrinsic to the physical kinetic theory of gases model but must be simulated for the pseudo-2D model with the assistance of a derivation.

The cross-section of the particle is defined as the area within its interaction radius r, $\sigma = \pi r^2$. This provides a basis for calculating the interaction volume that the particle will pass through if moving at velocity, v, over a time step, dt:

$$V = \sigma v dt. \tag{12}$$

This is visualised in Figure 8. Multiplying this volume with the number density of the gas, n, we get the number of collisions for the particle, dN, when travelling distance vdt:

$$dN = n\sigma v dt \tag{13}$$

This can be rearranged for the rate of collisions per time step or collision frequency f:

$$f = \frac{dN}{dt} = n\sigma v. \tag{14}$$

For the purposes of the pseudo-2D model, an absolute value of collision frequency is not necessary. Instead, a relative collision frequency is sufficient to maintain the relationship between velocity and collision frequency, defined as the ratio of collision frequencies between a particle and a reference:

$$\frac{f}{f_{ref}} = \frac{n\sigma v}{n\sigma v_{ref}} = \frac{v}{v_{ref}}. \tag{15}$$

The simplification arises from the fact that the particles are identical and in the same system, and thus have the same crosssection and number density. The resulting linear relationship was incorporated into the pseudo-2D model to simulate the collision frequency property.

The next simulated property was the 2D elastic collision, though implementation of this was much simpler owing to a key understanding of the elastic collision described in the previous section. This was that the single parameter that controls the collision dynamics of a 2D or 3D elastic collision is the collision vector between the contacted particles which can be succinctly described by the contact angle between the two particles illustrated in Figure 9.

4.1. Model & Method

The pseudo-2D kinetic theory of gases model was built using Python, with identical scientific libraries to the 2D Kinetic theory model in addition to h5py for HDF5 data storage/compression, and multiprocessing for batch running. The simulation is initialised with n agents, each with identical kinetic energy and mass, a uniformly randomised direction of velocity in 2D, and a selected collision mechanism. Each of the agents are stored within a scheduler which randomises the order in which agents are activated at each time step, cycling through all of them consecutively. The behaviour of an agent, when activated directly, is depicted graphically in Figure 10. Once activated, an agent will calculate its collision frequency based on its velocity and a reference velocity and the formula of Equation 15; using $v_{ref} = 1$ and $f_{ref} = 1$ for these simulations. For each multiple of the v_{ref}, a collision occurs, remainders are taken as probabilities, implemented through a random number generator. The agent will then undergo the number of collisions determined by their collision frequency f, selecting a random agent from the population for each repetition, then undergoing a 2D elastic collision randomised by contact angle or an alternative collision mechanism. For comparison, a collision mechanism involving the random exchange of energy was used. After all agents had been activated by the scheduler, the simulation data is collected and stored, followed by the next time step until the simulation is complete.

Mean final distributions and relaxation times were taken from the energy/speed distributions of the final 1,000 steps for each run, with each run being repeated 10 times and the mean final distributions being averaged over. Each dataset took roughly 12 hours with parallelisation using multiprocessing. Furthermore, relaxation was measured using relative entropy utilising a rolling average distribution over a 10-step window and an averaged distribution of the final 1,000 steps. The results presented utilise the following model parameters: N (10000) steps, n (1000) agents, n (1) initial kinetic energy and mass = 1. Source code is available with instructions in Appendix 8.9.

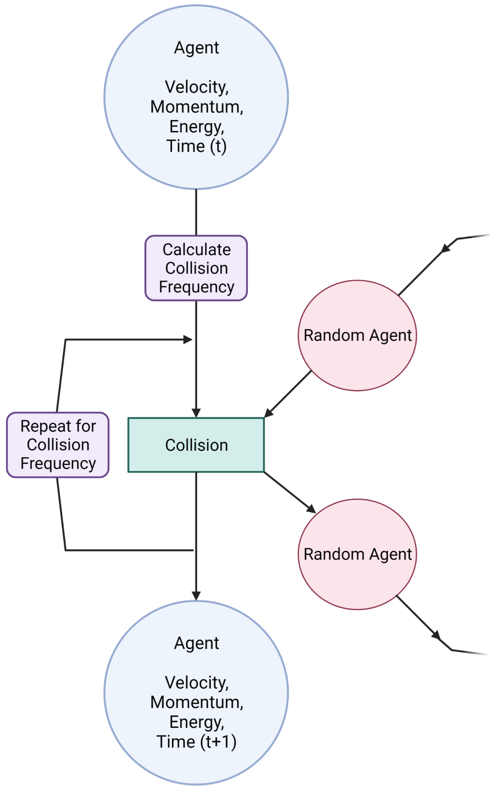

Figure 10: Flowchart depicting the logic and methods of an agent in the pseudo-2D model when activated [13].

4.2. Results & Discussion

An averaged speed distribution of the final 1,000 steps of the full pseudo-2D model was fitted with a Maxwell-Boltzmann speed distribution and shown in Figure 11. The quality of fit demonstrates the validity of the pseudo-2D model as a good approximation of the 2D equivalent. Further study into the effect of collision frequency, 2D elastic collisions, and the randomised scheduler was carried out through a comparison of speed distributions.

The effect of collision frequency can be visualised by comparison of the final speed distributions of simulations with and without collision frequency illustrated in Figure 12a. Both distributions resemble that of the Maxwell-Boltzmann distribution, with a slight contraction for the model with collision frequency. This effect was as expected, with redistribution of probability from higher energy particles to the rest of the system. The limited impact of collision frequency on the resulting distribution suggests that it is not the dominant factor in the formation of the Maxwell-Boltzmann distribution. Moreover, the calculation of collision frequency was based on a reference velocity of 1 which was chosen arbitrarily, potentially causing the difference in shape. It may be relevant to calculate a realistic collision frequency for a system determining number density, cross-section, etc. The low reference velocity paired with the random activation of the pseudo-2D model had the consequence that the whole of the population underwent at least 1 collision within the first time step. Effectively removing the physical limitations to diffusion through the system, allowing instant relaxation.

A similar comparison was carried out between 'Kinetic' 2D elastic collisions and 'Simple' uniform random energy exchange depicted in Figure 12b. Evidently, the two distributions are identical. This is a revealing result as it has the implication that the 2D elastic collision for 2 identical particles, and by extension a randomised elastic collision for any number of dimensions, is equivalent to a random uniform exchange of energy. In retrospect, this is a trivial observation as the two particles having the same mass implies equal momentum and energy exchange. Future work could involve developing models with non-identical particles which may draw similarities to different economic systems, for example, representing different sizes of companies.

Despite the limited effectiveness of collision frequency and 2D elastic collisions, these were

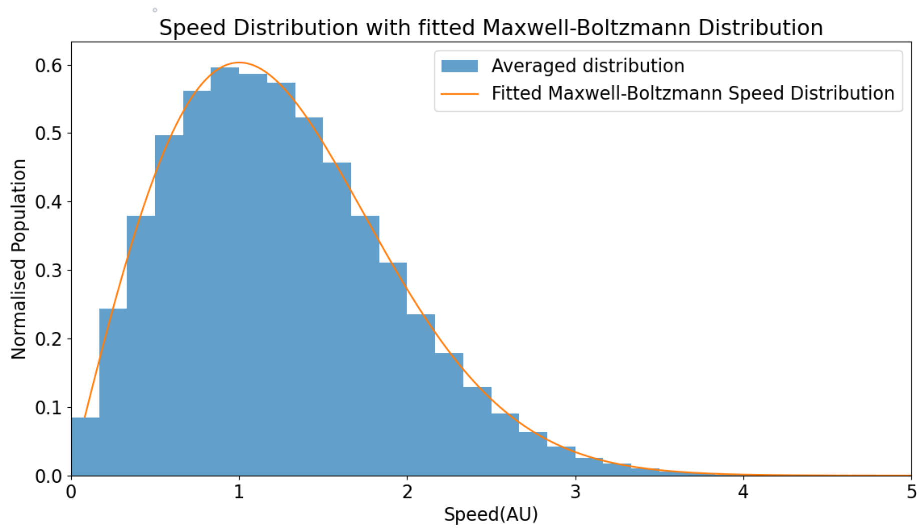

Figure 11: Histogram showing average speed distribution of final 1,000-steps of full pseudo-2D model fitted with a Maxwell-Boltzmann speed distribution.

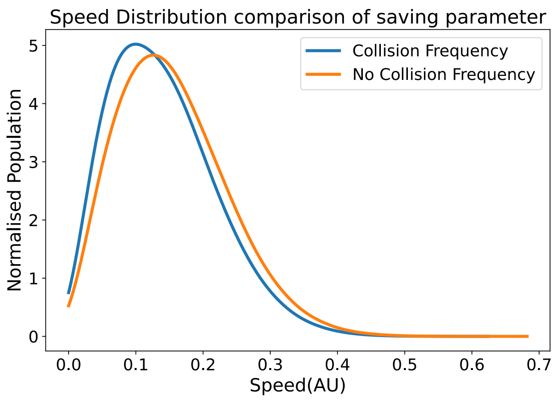

(a) Comparison of speed distributions with and without collision frequency.

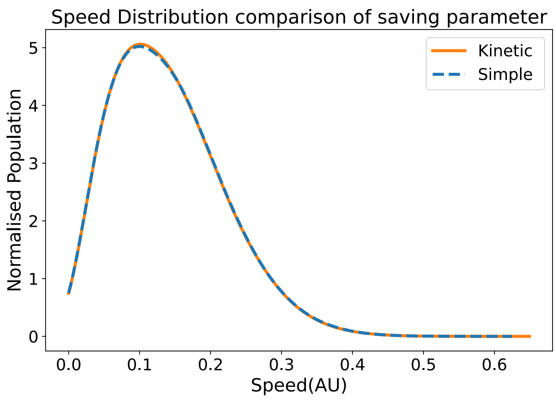

(b) Comparison of 'Kinetic' elastic 2D collisions, and 'Simple' energy exchange mechanisms through speed distribution.

Figure 12: Speed distributions of the pseudo-2D model comparing 2 key model parameters.

both included in the following models to ascertain any relevance to the economic adaptations.

5. Introduction of Saving Parameter to Pseudo-2D Model

After verifying the validity of the pseudo-2D kinetic theory of gases model as a valid kinetic theory model through its Maxwell-Boltzmann distribution in speed, the model was applied to the study of wealth distribution. The direct analogy was made to consider particles as traders and the collisions between them as transactions of energy or money within a market. This application is the basis of a category of economic models known as kinetic theory usually referring to the random selection of interaction partners between agents. Through a literature review, a paper of interest "Pareto law in a kinetic model of a market with random saving propensity" was identified [20]. In this paper, a saving parameter was introduced into the model producing interesting behaviour in the resulting wealth distributions. This inspired incorporation of a saving parameter into the pseudo-2D model. The results and effects of the collision frequency and elastic collision features of the pseudo-2D model are described, as well as the economic implications of the results.

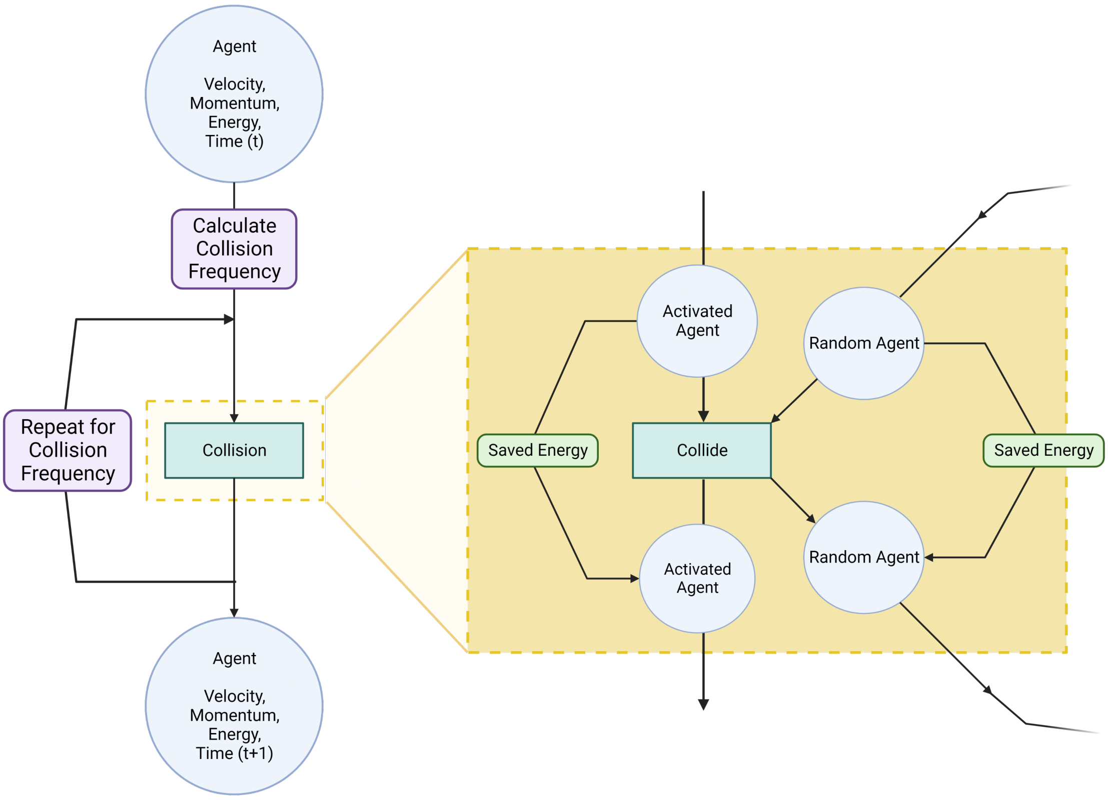

Figure 13: Flowchart depicting the logic undergone by an agent in the full pseudo-2D model with saving parameter when activated.

5.1. Model & Method

This model is built entirely upon the pseudo-2D model with the addition of a saving parameter. The saving parameter, λ, is defined during the initialisation of the agent as the fraction of money which the agent will save from being involved in a collision/transaction and then returned to the agent after the collision. The full logic of the agent is depicted in Figure 13. Two variations of the model were assessed: Homogeneous saving parameter for all agents (i.e. all agents have a saving parameter of 0.5), and uniform heterogeneous saving parameter range (i.e. uniform distribution of saving parameter between 0.0 - 1.0). Source code is available with instructions in Appendix 8.9. Due to longer relaxation times, simulations were run for 100,000 steps, and all other properties of the simulation and traders were identical to the pseudo-2D model, as well as analysis methods.

5.2. Results & Discussion - Homogeneous saving parameter

A linear scale graph of the resulting wealth distributions for saving parameters 0.0 for no saving, 0.5 for some saving, and 0.9 for substantial saving are depicted in Figure 14. In the case of no saving, the energy distribution resembles the Maxwell-Boltzmann energy distribution for a 2D system as expected. In the cases with some form of saving parameter, two main features are observed. A narrowing of the wealth distribution and shifting of the peak away from 0 to higher wealth, scaling with greater λ. The wealth distribution decays exponentially, with a lesser degree on the higher wealth tail. The peak also appears to tend asymptotically towards the value of the starting money $= 1$ as the λ is increased to 1. This can be understood as the saving parameter limiting the maximum money lost and gained through an interaction, thus creating a bias towards energy conservation, increasing with λ.

The source of these distortions could be understood through the development of a balance equation relating the rate of change of the energy distribution to the rate of energy transfer

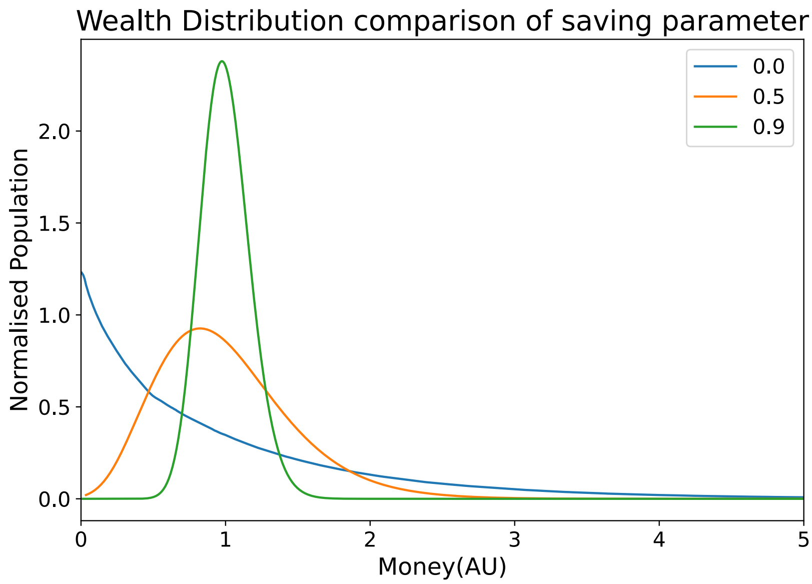

Figure 14: Comparison of wealth distribution of full pseudo-2D model with 3 different homogeneous saving parameters: No saving (blue 0.0), some saving (orange, 0.5), and substantial saving (green, 0.9).

between particles in the system. For the kinetic theory of gases, this is referred to as the Boltzmann equation. Incorporation of the saving parameter would add an additional component to the energy transfer mechanism thus producing an adjusted balance equation. Further comment would require an in-depth study that is outside of the scope of this project but would be of potential interest for future work.

Comparison of the effects of collision frequency and kinetic collisions were not meaningful with relaxation times for these distributions being instant similar to the standard pseudo-2D model.

5.3. Results & Discussion - Heterogeneous saving parameter

If considering a real economic system, a saving parameter would be heterogeneous within the population. This was incorporated as a uniform spread of saving parameter, although a non-uniform spread may be of interest for further study. The chosen saving parameter ranges were: 0.0 - 0.5(lower), 0.5 - 1.0 (upper), and 0.0 - 1.0 (full), with final wealth distributions compared in Figure 15, using log scale due to the nature of the resulting distributions. For the lower saving parameter range, a wealth distribution similar to that of the homogeneous saving parameter is seen, This is more clear in the linear plot, available in Appendix 8.7. Whereas the upper and full saving parameter ranges exhibit a much more skewed distribution towards higher wealth, showing a somewhat linear relationship for above 10^0 money - this implies a power law (x^α) relationship due to log axes. Power law tails were fitted giving exponents: upper $\alpha = -3.52 \pm 0.05$, full $\alpha - 2.52 \pm 0.02$. Sampling errors are present in the tail of the distribution. Consequently, the power law exponents may not be true to the system. Sampling errors were a primary challenge for this model as computing power was limited. Further study would ideally acquire access to a computer cluster or some other more powerful resource for running a larger number of simulations with more complex models.

In the context of economics, power laws are common phenomena, seen in wealth distributions of societies throughout history and are referred to specifically as Pareto law distributions. The consensus of the underlying cause of these distributions is that richer individuals enact

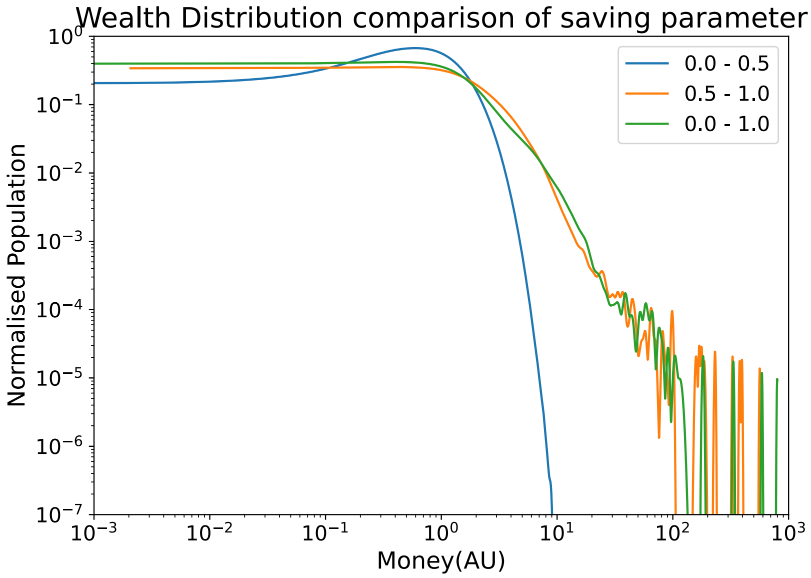

Figure 15: Comparison of wealth distribution of full pseudo-2D model with 3 different heterogeneous saving parameter ranges: lower (blue, 0.0 - 0.5), upper (orange, 0.5 - 1.0), full (green, 0.0 - 1.0).

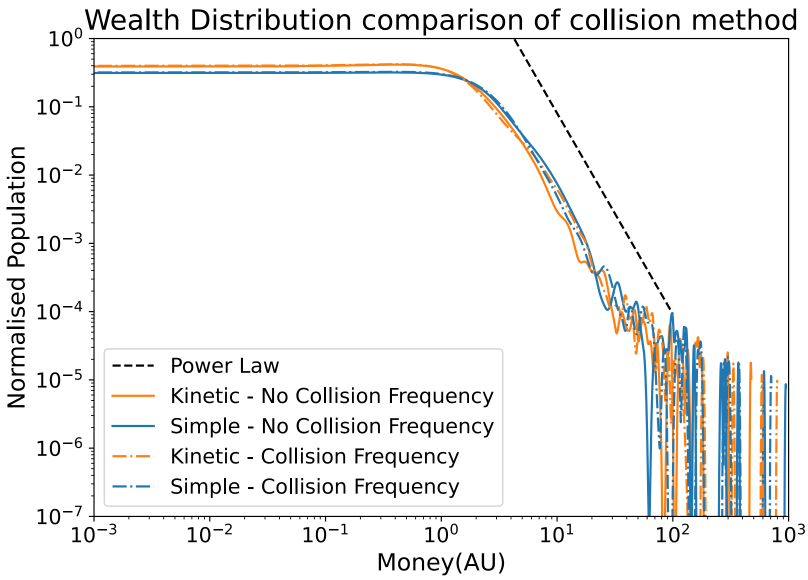

Figure 16: Wealth distributions of pseudo-2D model with full heterogeneous saving range (0.0 - 1.0) comparing effects of collision frequency and 2D elastic collisions, with additional fitted power law to kinetic with collision frequency model with exponent $\alpha = 2.52 \pm 0.02$.

mechanisms to protect their wealth; still interacting and exchanging wealth with society but risking a smaller proportion [21]. In the heterogeneous pseudo-2D model, the saving parameter appears to implement this. This can be intuited as differences in saving parameter encoding a bias in transactions towards individuals with greater saving parameter, who make more profit from their transactions and could be described as more profit-oriented. This can be related to businesses in a society constantly increasing profit margins relative to other individuals in society whether they be people or businesses. As a consequence, an unequal Pareto law wealth distribution is observed in the heterogeneous saving parameter model.

The prevalence of power laws in nature is also extensive. For example, in relativistic gas collisions, when high-energy, fast-moving particles collide with slow, low-energy particles, only a small fraction of their energy is exchanged relative to the slow particle, thus producing power law distribution seen in cosmic ray energy spectra [22]. Further examples exist in plasma and non-ideal gas systems, for example, driven inelastic gas simulations [23, 24]. Future work for this project could include the study of these systems and through acquiring a greater understanding of the physical saving parameters present in these systems, additional inferences could be made on the source and features of these Pareto law wealth distributions within society.

The results from this model offer a further insight. Even in societies where all individuals are given identical initial wealth, starting from an equal footing, as a result of the inherent heterogeneity of transactions and business within a capitalist society, unequal wealth distribution can be considered an inevitable result. This suggests that reducing inequality is more dependent on reducing the (unequally distributed) profits of businesses within that society rather than providing all individuals with an equal monetary starting point. Evidenced by the reduced inequality found in the lower saving parameter range simulations, where the power law wealth distribution was not the dominant feature, and wealth was more distributed towards the lower ranges.

The effects or lack thereof of the collision frequency and mechanism for heterogeneous saving parameter on the final wealth distribution are illustrated in Figure 16, where a comparison is made for the full saving parameter range (0.0 – 1.0). Similar to the base pseudo-2D model, the differences are negligible in the final distribution, with most tails ($10^0 - 10^2$) having an exponent around 2.50, exact values available in Appendix 8.8. Though the accuracy of these is questionable due to the inconsistent gradient as a result of insufficient sampling. Similar results were observed for the other saving parameter ranges. However, studying the relaxation of these wealth distributions revealed some differences as depicted in Figure 17. The collision frequency had the effect of vastly reducing the relaxation time of the distribution. This can be understood by considering that the collision frequency increases the number of transactions undergone by richer agents such as those with higher saving parameter who are on average gaining more wealth from collisions than lower saving parameter agents. It is thus clear that the incorporation of collision frequency only further accelerates the rate at which they gain wealth. Assuming the relaxation is dependent on the formation of this unequal power law distribution, this effect can be attributed to the shorter relaxation for collision frequency simulations. An example of an isolated averaged relaxation with variance is provided in Appendix 8.6 for reference.

Through modelling societies as particles of an ideal gas, randomly transacting money through collisions, these pseudo-2D models, with the incorporation of saving parameters, provide an insightful perspective into the source of inequality within society, as well as how this can be reduced.

6. Conclusions

Econophysics has been and will continue to be a vital field in economics. Attempts to model economic systems generally face a trade off between replicating specific features of real-world processes and being analytically tractable in order to produce computable results. Agent-based modelling can provide an alternative to this approach by modelling economic systems as a large

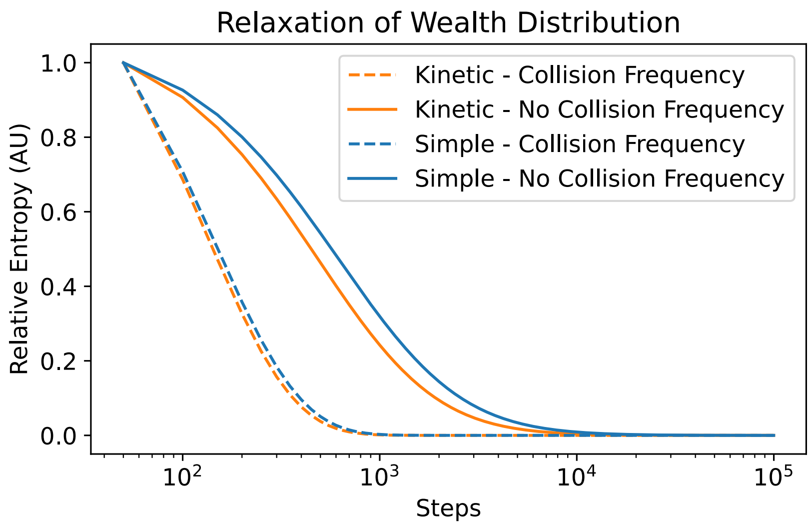

Figure 17: Averaged relaxation of pseudo-2D model with full heterogeneous saving range (0.0 - 1.0) comparing effects of collision frequency and 2D elastic collisions.

number of economic agents, with potentially more complex behaviours, interacting to produce collective phenomena and results without the need for analytical methods. Furthermore, the structures of many economic systems are analogous to that of agent-based models, making them well-suited to study using these techniques. This project involved the development of several agent-based models, not to attempt to replicate the detailed empirical reality of the economic world, but designed in ways that exhibited non-trivial emergent properties that were analogous to and offered insights into real-world economic phenomena, specifically stock price fluctuations and wealth distributions.

Brownian motion is one of the most prominent concepts in Econophysics, describing the random movement of particles in a system with a number of similar features to economic systems, most popularly stock price fluctuations. A model of this was developed and explored, identifying Geometric Brownian Motion as a popular foundation for a number of economic models of a physical phenomenon to economics, for example, the famous Black-Scholes model of option pricing [5]. The relevance of Brownian motion to economics inspired this study of the random collisions of particles that give rise to its behaviour through development of a Kinetic Theory of Gases model.

A 2D Kinetic theory of gases model was developed to understand the underlying causes of the random behaviour of gases. The model was verified through the characteristic Maxwell-Boltzmann distribution, serving as a fundamental example of modelling large systems from the simple behaviour of a number of interacting agents. This physical model was identified to be inflexible for application to economic systems. An adapted pseudo-2D model was therefore developed to extract some of its flaws whilst attempting to retain the reality of the kinetic theory. The pseudo-2D kinetic theory of gases model was found to be consistent with the previous geometric kinetic theory model, with energy and velocity distributions resembling Maxwell-Boltzmann distributions. By reconsidering collisions as transactions, and energy as wealth, the model was adapted for the study of wealth distributions. Taking inspiration from literature, homogeneous and heterogeneous saving parameters were introduced to the pseudo-2D model, significantly impacting the resulting wealth/energy distributions.

Homogeneous saving parameters led to narrow wealth distributions with less inequality, as the uniform saving parameter within the population made agents conserve their wealth in transactions. Heterogeneous parameters introduced unfairness into the system, with higher saving parameter actors profiting over lower saving parameter actors, resembling businesses and/or individuals within society competing with each other. Reduced saving parameter ranges (0.0 -0.5) produced less unequal, shifted Maxwell-Boltzmann-like wealth distributions similar to the homogeneous saving parameters, while higher ranges produced steep Pareto/power law distributions with extensive inequality. These findings demonstrate that large disparities in saving parameter, resembling greater profit orientation of actors (individuals or businesses) within a population will naturally lead to unequal Pareto law wealth distributions regardless of initial wealth. This implies that reduction of inequality is controlled by the degree of profit orientation within a society, not by the initial wealth of individuals. Collectively, these results provide an alternative perspective on the source of inequality within society, with potential application for economic policy designed to reducing it.

Further research in this area could explore a number of areas highlighted in this thesis including developing a more accurate understanding of the kinetic theory of gases model with saving parameter incorporation, perhaps approaching the problem through the balance equation describing energy transfer within the system through the Boltzmann equation, adapting energy exchange for saving parameters. Additionally, developing models of non-ideal and non-identical particles with different mass, shape, etc, and exploring their behaviours, particularly in the context of wealth distributions. Additionally, further study of physical systems that have similar behaviour to the heterogeneous saving parameter models could provide more insights towards understanding Pareto distributions. For example, driven systems to model the constant flow of wealth into economies, and the interactions of relativistic gas models.

7. References

[1] Mantegna R N R N and Stanley H E H E 2000 *An introduction to econophysics : correlations and complexity in finance* (Cambridge University Press) ISBN 0 521 62008 2

[2] Hetherington N S 1983 *Journal of the History of Ideas* **44**(3) 497 ISSN 00225037

[3] Mandelbrot B 1963 *https://doi.org/10.1086/258792* **71**(5) 421–440 ISSN 0022-3808

[4] Peters O and Gell-Mann M 2016 *Chaos: An Interdisciplinary Journal of Nonlinear Science* **26**(2) 023103 ISSN 1054-1500 URL `https://aip.scitation.org/doi/abs/10.1063/1.4940236`

[5] Chakraborti A, Toke I M, Patriarca M and Abergel F 2011 *Econophysics review: II. Agent-based models* vol 11 (Taylor & Francis)

[6] Carrère C, Mrázová M and Neary J P 2020 *The Economic Journal* **130**(628) 880–910 ISSN 0013-0133 URL `https://academic.oup.com/ej/article/130/628/880/5815071`

[7] Chen Z 2001 *arXiv preprint quant-ph/0112156*

[8] PhysicsWorld 2023 Financial rollercoaster: The ups and downs of ultralong-term bonds

[9] Axtell R L and Farmer J D 2022 *Journal of Economic Literature*

[10] Sornette D 2014 *Reports on progress in physics* **77** 062001

[11] Einstein A 1905 *Investigations on the theory of the Brownian movement*

[12] Clark P 1989 *Determinism, Probability and Randomness in Classical Statistical Physics* (Springer, Dordrecht) URL `https://link.springer.com/chapter/10.1007/978-94-009-3025-4_8`

[13] BioRender 2023 Diagrams made with biorender Website URL `https://biorender.com/`

[14] et al L C N 1995 *Journal of Fluid Mechanics* **282** 373–403 ISSN 1469-7645

[15] Shreve S E *et al.* 2004 *Stochastic calculus for finance II: Continuous-time models* vol 11 (Springer)

[16] Cont R 2007 *Long memory in economics* 289–309

[17] Brush S G 2003 *Kinetic Theory Of Gases, The: An Anthology Of Classic Papers With Historical Commentary* vol 1 (World Scientific)

[18] Landau L D and Lifshitz E M 1976 Theoretical physics, vol. 5: Statistical physics

[19] Schroeder D V 1999 An introduction to thermal physics

[20] Chatterjee A e a 2004 *Physica A: Statistical Mechanics and its Applications* **335** 155–163

[21] Drăgulescu A e a 2001 *Physica A: Statistical Mechanics and its Applications* **299** 213–221

[22] Modanese G 2016 *Physics Letters A* **380** 29–32

[23] Newman M E 2005 *Contemporary physics* **46** 323–351

[24] Thurner S, Korbel J and Hanel R 2021 *New Journal of Physics*

[25] Pons O 2020 *Probability and Stochastic Processes: Work Examples* (World Scientific)

8. Appendices

8.1. Derivation of Maxwell-Boltzmann Energy Distribution in 2D

Below is a derivation of the Maxwell-Boltzmann Energy Distribution in 2D from the speed distribution, beginning with:

$$P(v) = \left(\frac{m}{\pi k_b T}\right) v exp\left(-\frac{mv^2}{2k_b T}\right). \tag{16}$$

Utilising the following mathematical relation for change of variables

$$P(E)dE = P(v)dv, \tag{17}$$

then finding the relationship between dv and dE using the kinetic energy relation $E = \frac{1}{2}mv^2$:

$$dE = d(\frac{1}{2}mv^2), dE = mvdv. \tag{18}$$

Subbing this in to Equation 17 and rearranging gives

$$P(E) = \frac{P(v)}{mv}, \tag{19}$$

which when fully expanded gives the Maxwell-Boltzmann Energy distribution for 2-Dimensions as required

$$P(E) = \frac{mv}{k_b T} exp\left(-\frac{E}{k_b T}\right)\frac{1}{mv} = \frac{1}{k_b T} exp\left(-\frac{E}{k_b T}\right). \tag{20}$$

8.2. Relaxation of 2D Gas Model

The relaxation of the velocity distribution was assessed using the relative entropy metric, with results depicted in Figure 18. It is worth noting that the relaxation time for the distribution was dependent on several initial parameters within the model, primarily on parameters affecting the average collision frequency of the system. However, since it was not pertinent to the project, it was not investigated further.

Visualisation in log axes demonstrates the power law relaxation, reaching a steady state within 100 steps. This relaxation was revealed to be variable depending on starting conditions of the model such as starting energies and length of the time step, two factors that affect the number of collisions per time step. As such, it was theorised that the relaxation time was related to the number of collisions per time step, which increased for faster agents and longer time steps.

8.3. Collision Prediction

Collision prediction was not incorporated into the 2D Gas model largely due to computational limitations. When predicting collisions, the paths of all agents must be calculated which is comparatively computationally expensive relative to the model used. Additionally, when predicting collisions, one then must consider the possibility of secondary collisions and ricocheting. This becomes an optimisation problem, for which the computational resources in this project were not sufficient, in addition to the decision that the approximate model used in this project was sufficient for its purpose; which was to better understand energy redistribution in the kinetic theory of gases.

8.4. 2D Gas Validity Check

A longer 5000-step simulation was run, and a final 1000-step averaged speed distribution was fitted with a Maxwell-Boltzmann speed distribution to further demonstrate validity. The resulting fit was overlayed atop a histogram of the final step speed distribution, as seen in Figure 19. This further reinforced the validity of this 2D kinetic theory of gases model.

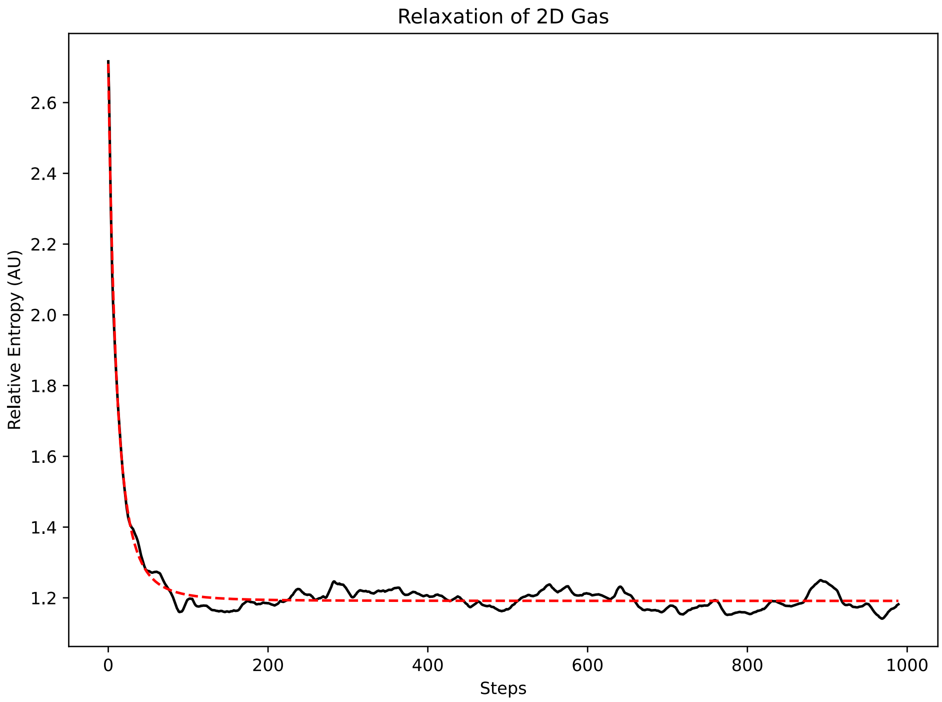

Figure 18: Relaxation of the speed distribution of the 2D Kinetic theory of gases model using the relative entropy distance metric.

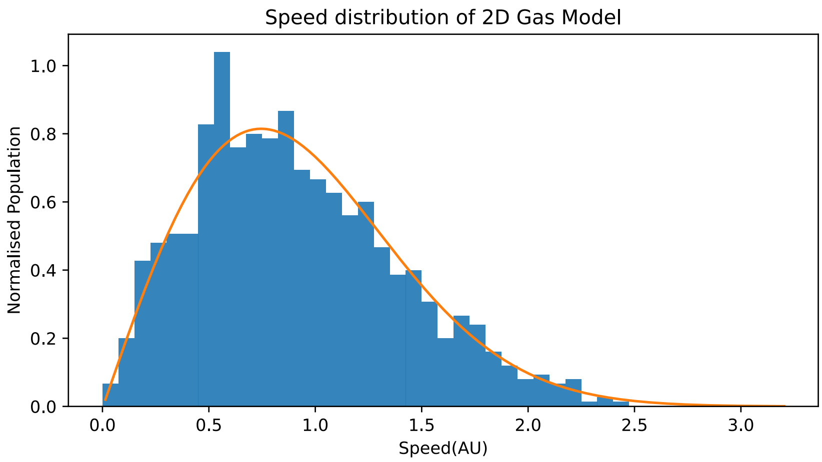

Figure 19: Histogram of final step speed distribution of a 5000-step 2D Gas simulation, fitted with Maxwell-Boltzmann speed distribution to final 1000-step averaged speed distribution

8.5. Relative Entropy

Relative entropy, also known as Kullback-Leibler divergence, is a distance metric used in statistics to measure the difference/similarity between two discrete probability distributions defined in the same sample space (range of x). Given two probability distribution functions, q and p, the relative entropy is defined as:

$$KL(p||a) := \int_{-\infty}^{\infty} p(x)log\left(\frac{p(x)}{q(x)}\right)dx \tag{21}$$

Where p and q must be defined over the same range of x. Note that this is not symmetric.
Its use originates from information theory, where information is conceptualised as being

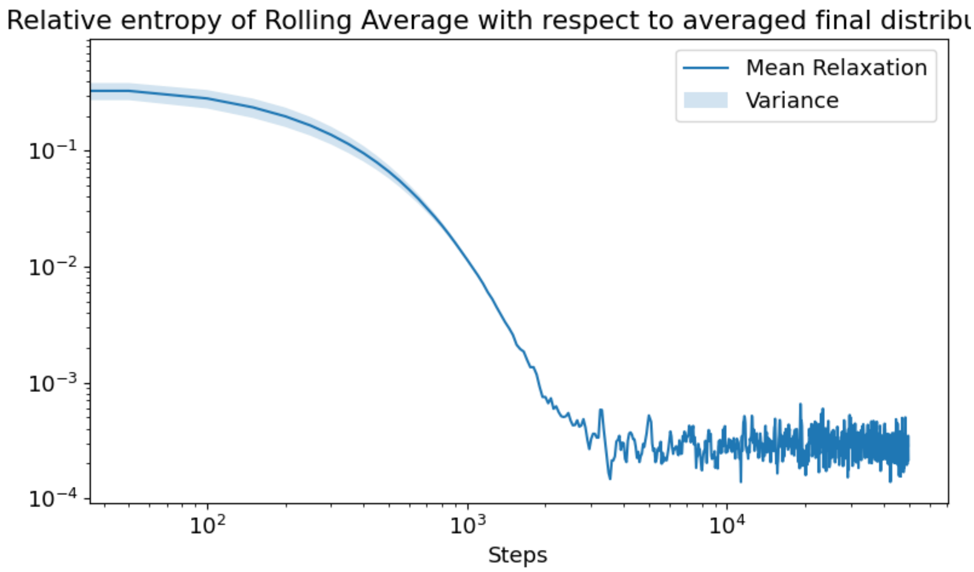

Figure 20: Example averaged relaxation of the wealth distribution with variance of the pseudo-2D heterogeneous saving parameter model with saving parameter range 0.0 - 0.5, 2D elastic collisions, and collision frequency, measured using the relative entropy distance metric.

equivalent to entropy more accurately termed Shannon entropy. Specifically, Shannon entropy is defined as the measure of the amount of uncertainty in a set of possible outcomes, often used to quantify the amount of information that is transferred by a message or signal. Intuitively this says that for a message containing lots of information, the entropy of the message is high, whereas a message conveying a small amount of information has low entropy [25].

8.6. Example Relaxation of Heterogeneous Saving Parameter Model

An example of an averaged (over 10 runs) relaxation of a heterogeneous pseudo-2D saving parameter is depicted in Figure 20.

8.7. Lower Saving Parameter Range Wealth Distribution

Depicted in Figure 21, is the linear plot of lower saving range, showing peaked behaviour similar to wealth distributions of homogeneous saving parameter range.

8.8. Power Law Exponents for Pseudo-2D Heterogeneous Wealth Distribution Feature Comparison

The power law tails of the pseudo-2D heterogeneous, full saving range (0.0 - 1.0) wealth distributions were fitted within the range $10^0 - 10^2$, with results and errors tabulated in Table 1.

Table 1: Power Law Exponents for power law tails of the pseudo-2D heterogeneous, full saving range (0.0 - 1.0) wealth distributions.

	Collision Mechanism	
	Kinetic	Simple
Collision Frequency	-2.52 ± 0.02	-3.72 ± 0.08
No Collision Frequency	-2.94 ± 0.05	-2.56 ± 0.05

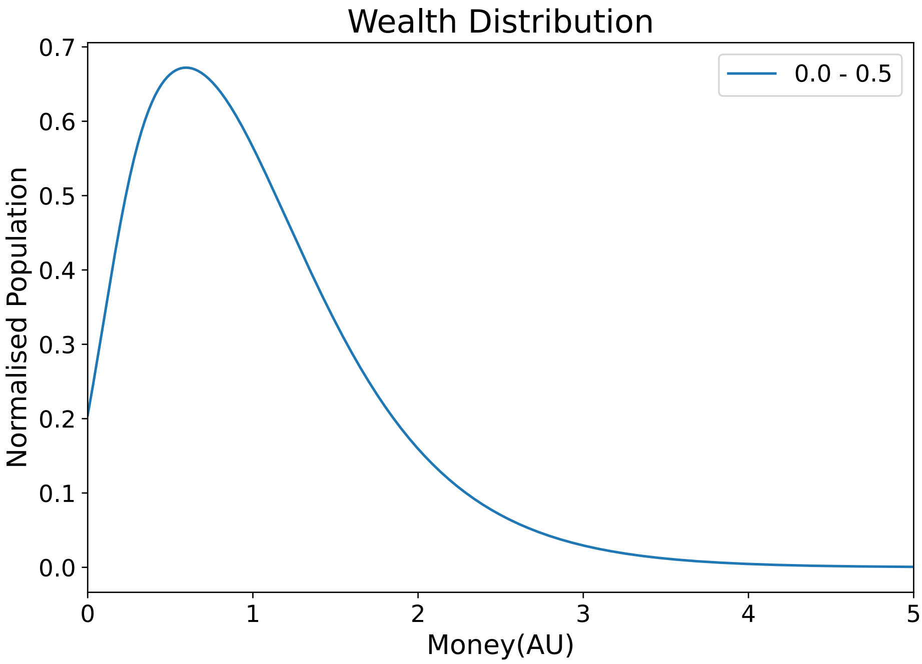

Figure 21: Linear plot of lower saving range (0.0 - 0.5) for heterogeneous pseudo-2D model.

8.9. Source Code

All source code is available in the GitHub repository available at the following address:https://github.com/2364784w/Agent-Based-Simulation-of-Particle-Collisions-and-Traders.

Code for Brownian motion models is accessible in file: /Brownian/Brownian.ipynb, for 2D Kinetic Theory of Gases in file: Mesa_2D_Gas_Model.ipynb, and for Pseudo-2D Model in file: Mesa_Pseudo_2D_Gas_Model.ipynb